Focussed on the Failure Analysis of Materials and Structures

Visual Abstract

The use of frictional and bonded contact models in finite element analysis for internal fixation of tibia fracture

Syifaul Huzni, Fikri Oktiandar, Syarizal Fonna, Fazal Rahiem, Lilis Angriani
Department of Mechanical Engineering, Syiah Kuala University, Aceh, Indonesia
syifaul@unsyiah.ac.id, fikriandar@mhs.unsyiah.ac.id, syarizal.fonna@unsyiah.ac.id, fazal_@mhs.unsyiah.ac.id, lilisangri@mhs.unsyiah.ac.id

ABSTRACT. Tibia is one of the bones that often fracture, generally occurring due to a car accident, falling from high places, work accidents, and sports injuries. Internal fixation is one of the solutions to repair broken bones. In some cases, internal fixation also failed to carry out its function, so the healing process was disturbed and did not run according to the plan. Factors that might interfere with the process can be analyzed using FEM. The objective of this study is to study the effect of the contact model used to model the connection between broken bones of the tibia, to stress distribution that occurs on fixation plate for walking conditions. Analysis was carried out by using ANSYS software with fine-sized tetrahedrons mesh. Two contact models were used. Namely, friction and bonded. The load amount used is based on the average weight of Indonesian Adults, i.e. 63 kg. The results of the analysis show that, for the friction contact model, higher stress is found in the middle area plate, adjacent to the broken location on the bone. Different results are found in the bonded contact model, larger stress occurs in the upper-end area fixation plate.

KEYWORDS. Tibia; Tibia fracture; Internal fixation; von Mises stress; Contact Models; Finite Element Method (FEM).

OPEN ACCESS

Citation: Huzni, S., Oktiandar, F., Fonna, S., Rahiem, F., Angriani, L., The use of bonded and friction contact models in finite element analysis for internal fixation of tibia fracture, Frattura ed Integrità Strutturale, 61 (2022) 130-139.

Received: 15.02.2022
Accepted: 19.04.2022
Online first: 28.04.2022
Published: 01.07.2022

INTRODUCTION

The tibia is the medial bone of the lower leg that connects the knee to the ankle and has the function of forming the leg skeleton and supporting body weight [1]. In some cases, the tibia is often fractured, generally occurring due to a car accident, falling from high places, work accident, and sports injuries [2]. The main factors that cause fracture are the torsion and the bending moment [3]. Fractured is a medical condition in which the continuity of bone tissue is damaged, resulting in fracture and loss of bone integrity.

Recovery of fractures in the tibia can be accomplished with internal fixation. Internal fixation is an orthopedic surgical procedure by placing implants in the form of plates and screws on the inside of the skin in the fracture area to stabilize the damaged bone tissue [4]. In some cases, internal fixation also failed to carry out its function, so the healing process was

disturbed and did not run according to the plan. Factors that might interface with the process can be analyzed using the Finite Element Method (FEM) [5]. Several studies have been performed related to Finite Element Analysis (FEA) on tibia fracture.

Hiranda, Afif [6] has examined the effect of element size on the result of the von Mises stress distribution in tibial fracture simulations where the results show that fine mesh is better to be used. Besides the mesh, there are other factors that affect the simulation results. The type of contact used in the fracture may also affect the distribution of the von Mises stress that occurs in the simulated internal fixation of tibial fracture. The objective of this study is to study the effect of the contact model used on the connection between broken bones of the tibia, to stress distribution that occurs on the fixation plate.

Although there are several types of materials that are often used for fracture implants, such as cobalt-chromium alloy [7, 8] and titanium-based alloy [9, 10, 11], stainless steel 316 was employed in this research for plate and screw to avoid the issue of the formation of chromium carbide which causes intergranular corrosion of the implant [12]. The load used refers to the average weight of an Indonesian male adult, which is 63 kg with loading conditions during walking.

MATERIALS AND METHODS

Internal fixation for a tibial fracture is shown in Fig. 1. The figure shows the geometry and dimensions of the tibia, along with the position of the plate in the middle of the tibia. The Plate has a length of 103 mm with a thickness of 3.8 mm. The screw used has a head diameter of 8 mm and a length of 28 mm [13, 14, 15]. The detailed dimensions of the plate and screw can be seen in Fig. 2.

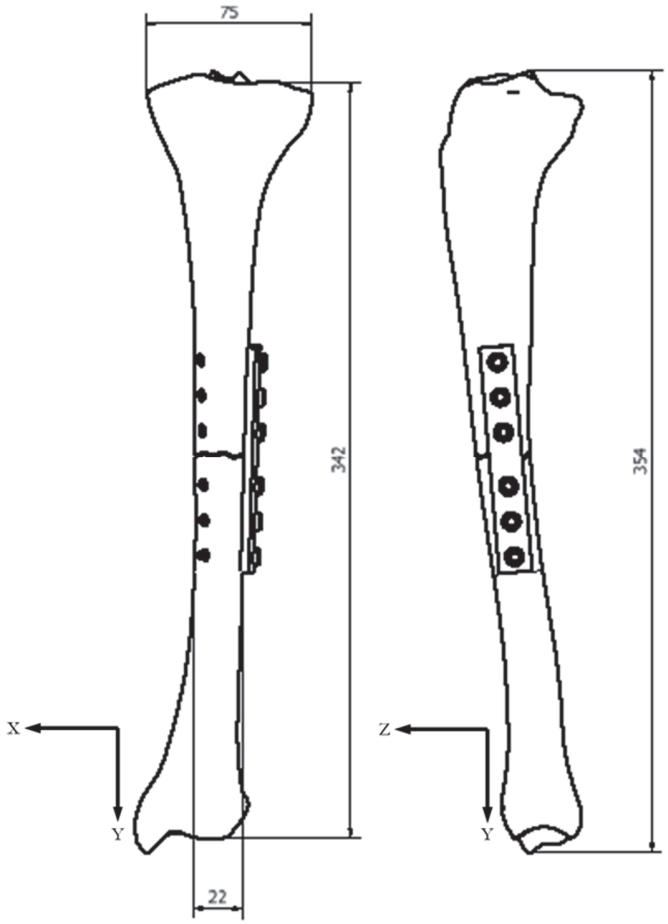

Figure 1: Internal fixation model for tibia fracture.

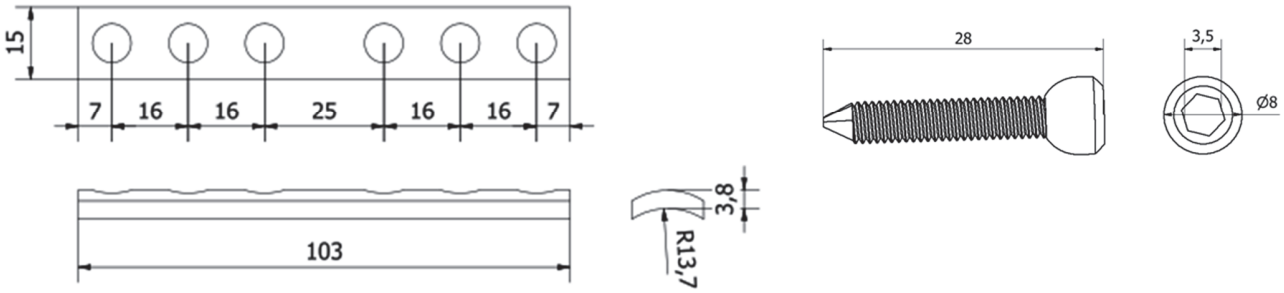

Figure 2: Plate and screw dimensions.

The type of material used for the plate and the screw is AISI 316 Stainless Steel. Stainless steel 316 is a material that is used because it can reduce the formation of chromium carbide which causes intergranular corrosion in implants [10-12]. The mechanical properties of stainless steel 316 are shown in Tab. 1. As for the tibia, the mechanical properties of the bone material used can be seen in Tab. 2.

AISI 316 Stainless Steel		
Yield Strength	205	MPa
Ultimate Tensile	515	MPa
Density	8000	kg/m^3
Elastic Modulus	193	GPa

Table 1: Mechanical properties of the AISI 316 Stainless Steel [16].

Tibia Bone		
Modulus Young	2.13	GPa
Poison's Ratio	0.3	-
Density	2000	kg/m^3
Shear Modulus	819.23	MPa

Table 2: Mechanical properties of the tibia [17].

BOUNDARY CONDITIONS

In this boundary condition setup (Fig. 3), the actual condition of the tibial fracture internal fixation model will be determined based on assumptions from various supporting literature. In this condition, the fixed support is still determined in section A and the load is given to sections M and L with the proportion of the load distribution being 60% in the medial (M) and 40% in the lateral (L) [18]. The load used in the simulation refers to the average weight of male Indonesian adults, which is 63 kg [19]. The mesh used is fine-sized tetrahedrons (Fig. 4), because this mesh is suitable for complex geometries [20].

The contact model condition between the plate and the tibia is frictional, and the contact model condition between the screw and the tibia is bonded. The coefficient of friction used in the frictional contact model is 0.2 [13, 21]. Meanwhile, the contact model that occurs between bones in the fracture area is varied with two types, namely bonded and friction. Variations in the contact model were performed to see the effect of the contact model on the stress distribution on the internal fixation model for the tibia.

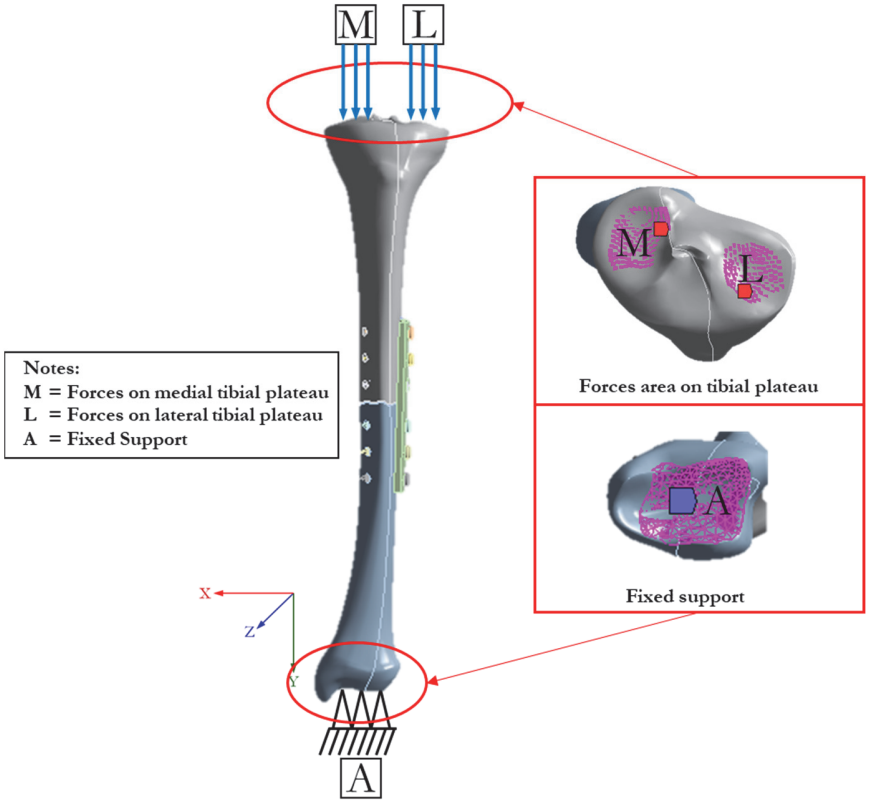

Figure 3: Boundary conditions setup.

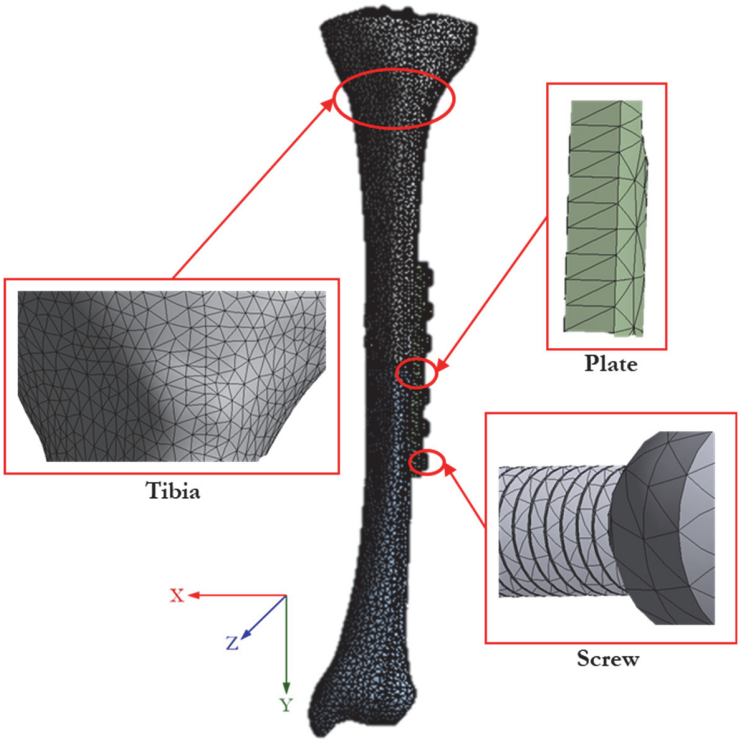

Figure 4: Meshing on internal fixation models for tibia.

LOADING CONDITIONS

In this work, the tibia model used is for the left leg. During walking, Fig. 5. The greatest load on the tibia occurs at 1.0 seconds when the leg with internal fixation is supported body weight.
The variations of the load on the tibia for walking conditions are shown in Tab. 3. Acting forces are defined as 3 components applied on the tibial: Fx, Fy, and Fz, Fig. 3.

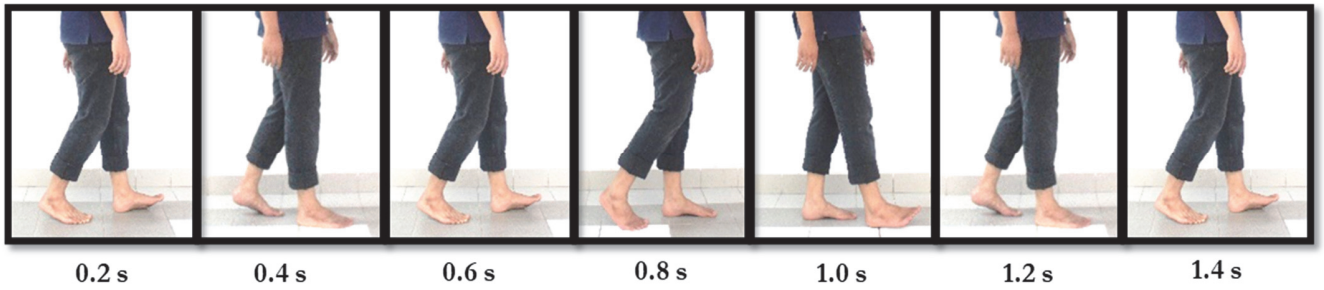

Figure 5: The position of the legs during walking for 1.4 seconds.

Time (s)	Fx (N)	Fy (N)	Fz (N)
0.2	-50.1	110.96	72
0.4	-19.19	591.24	69.33
0.6	-49.62	1193.4	-43.09
0.8	-16.07	1326.79	-66.32
1.0	11.64	1719.42	-4.2
1.2	-61.58	338.38	80.27
1.4	-33.08	63.75	88.74

Table 3: The force on the tibia during walking for 1.4 seconds [22].

RESULTS AND DISCUSSION

The results of the analysis to see the stress distribution on the tibia internal fixation model during walking 1.4 seconds from two different contact models were carried out using ANSYS based on the element method. Fig. 6 presents the contours of the von Mises stress distribution on internal fixation for the frictional contact model. It was observed that the stress distribution was focused on the center of the plate, adjacent to the broken location on the bone. This is clarified by Fig. 7, wherein from 6 points of stress magnitude taken at each time for 1.4 seconds during walking, it is seen that point 3 and point 4 have a higher stress magnitude than the other points.
Different results are found in the bonded contact model, Fig. 8. It can be seen that the stress distribution is focused on the upper end of the plate. This is then clarified in Fig. 9, it can be seen that point 1 has a higher stress magnitude than the other 5 points.
In addition to P1, 0.8 seconds and 1.0 seconds also have a higher von Mises stress distribution at P3 and P4 than other times. When the walking condition was at a time of 0.8 seconds, the position of the leg with the internal fixation on the tibia becomes a support for the body-weight so that it receives a high force. The high force causes a high-stress distribution in the center of the plate (P3 and P4).

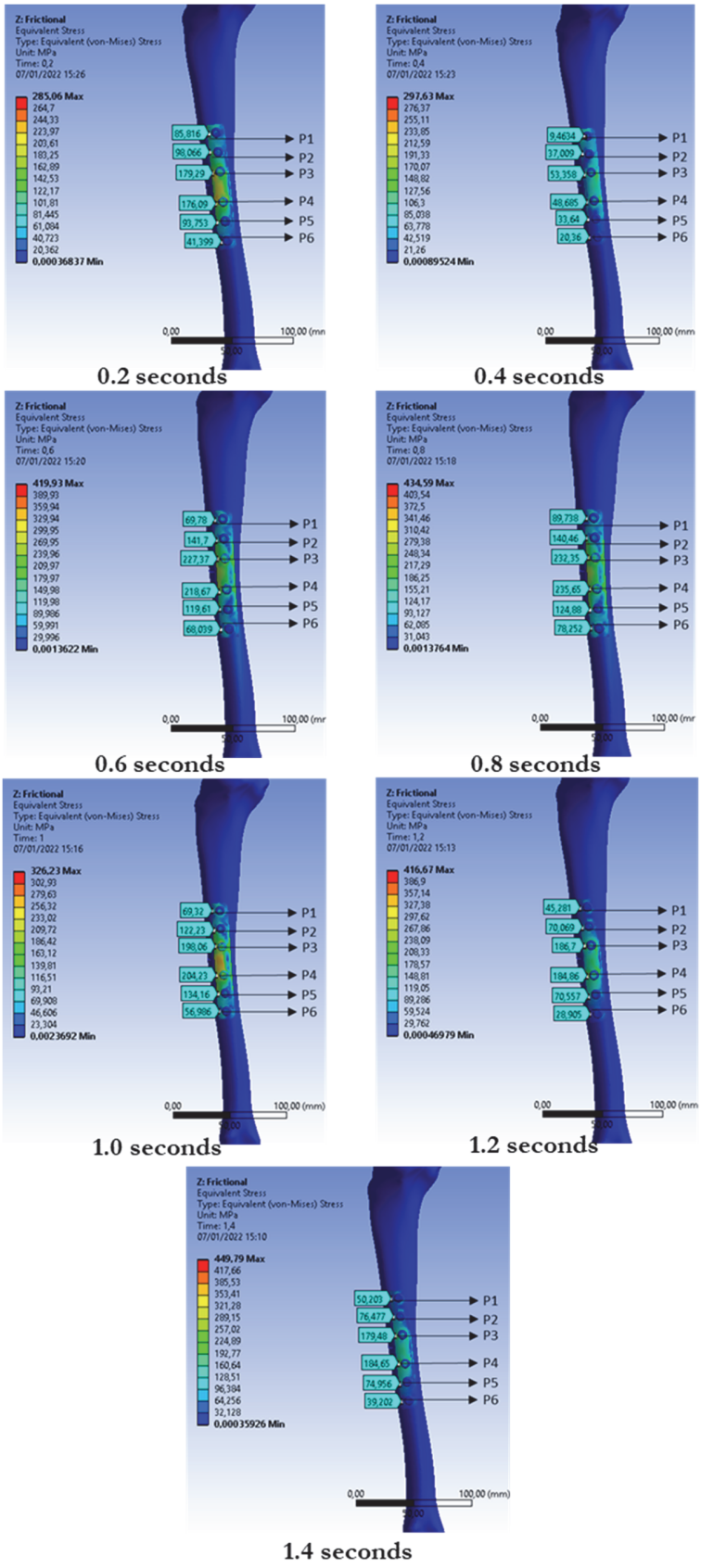

Figure 6: Von Mises stress distribution with a frictional contact model.

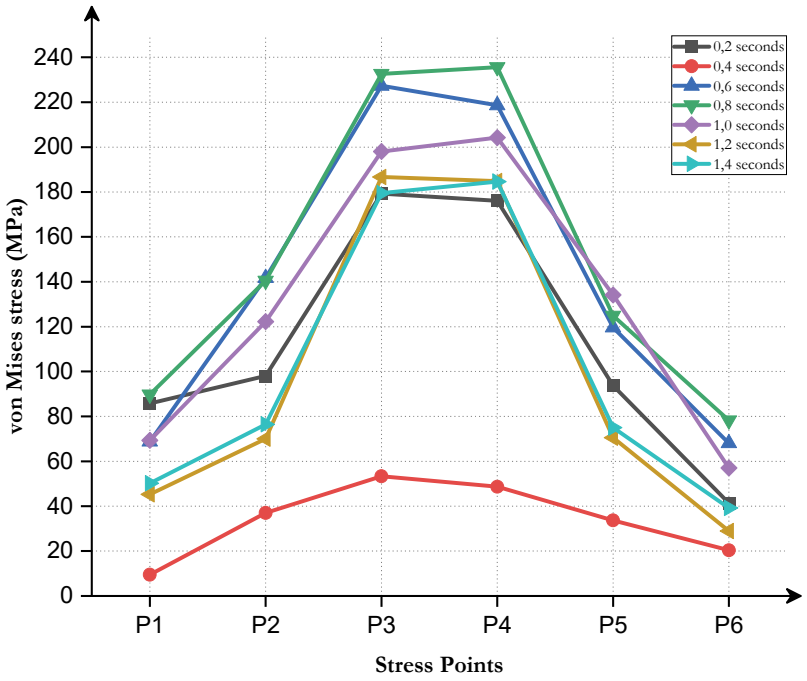

Figure 7: Von Mises stress magnitude at 6 points with a frictional contact model.

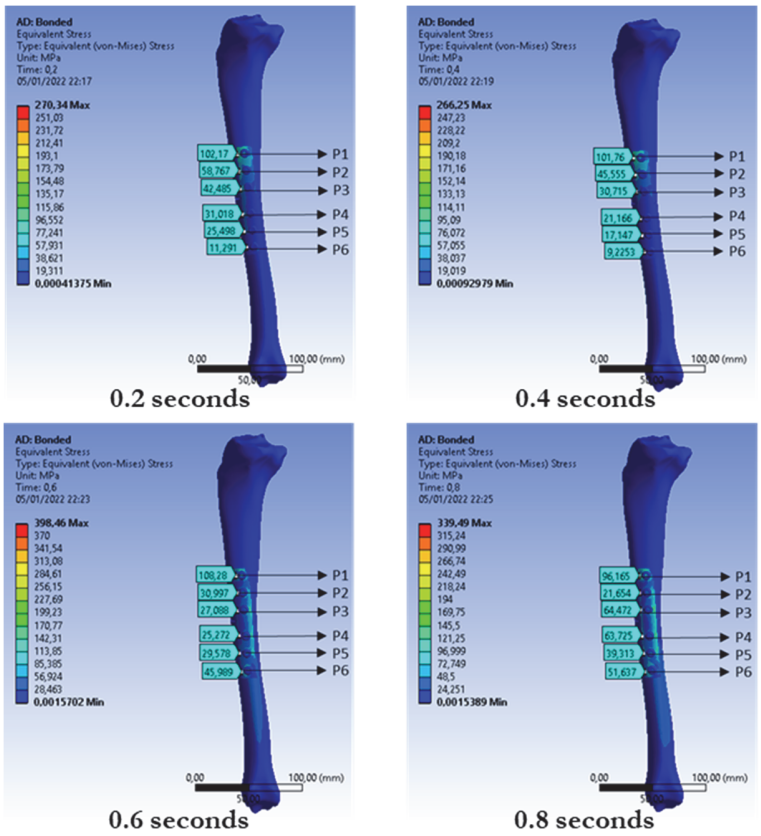

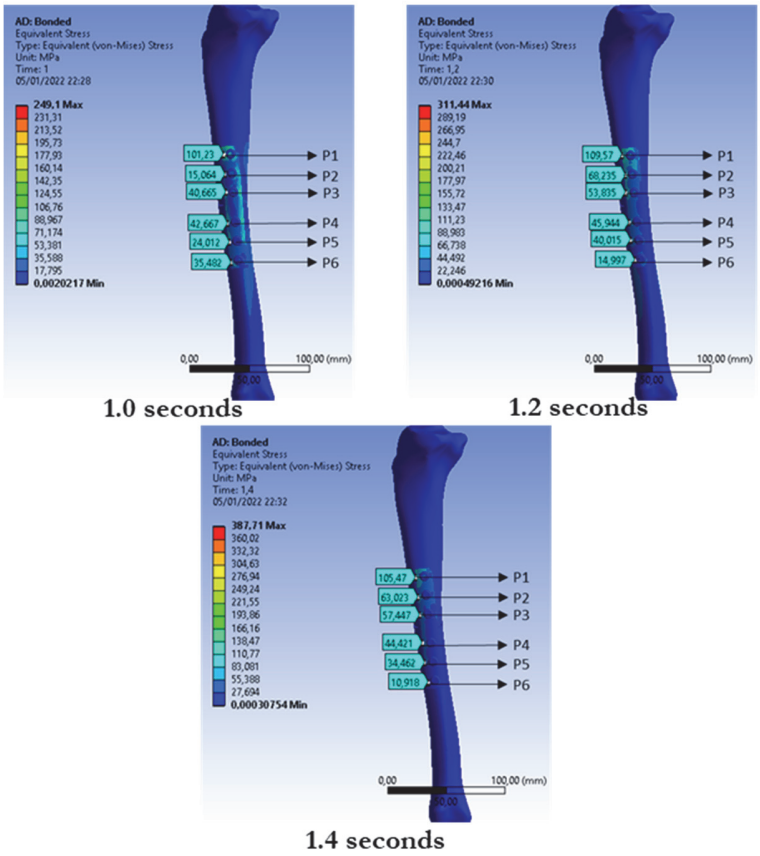

Figure 8: Von Mises stress distribution with a bonded contact model.

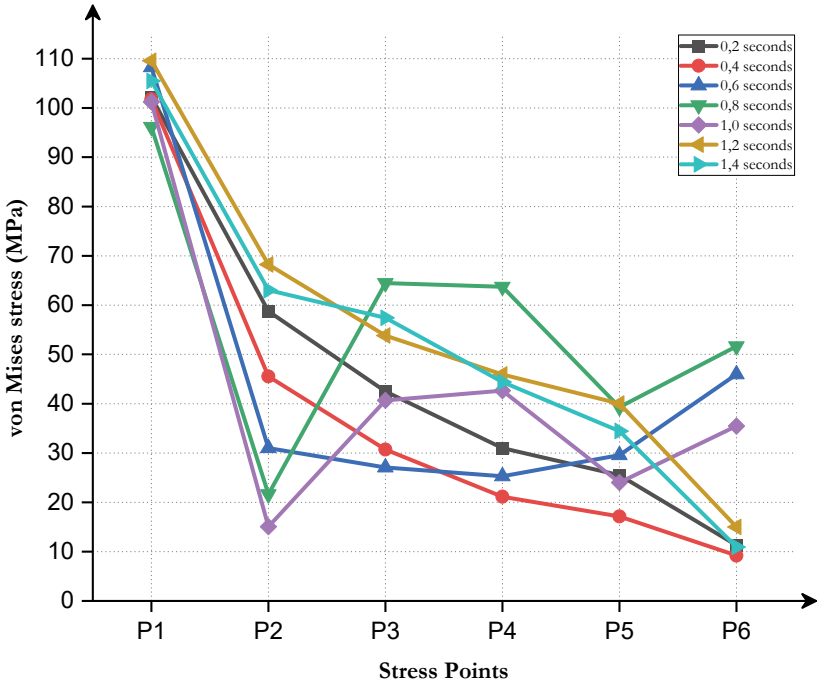

Figure 9: von Mises stress magnitude at 6 points with a bonded contact model.

From the results of the analysis on the internal fixation of the tibia for two contact models, it was found that the use of the frictional contact model in the simulation of the Finite Element Analysis (FEA) is suitable for the geometry model of the tibia with fractured. The bonded contact model is suitable for the geometric model in which the tibia has completely healed, but the internal fixation has not been removed.

Conclusions

In this study, the contact model has an influence on the results of the finite element analysis as the hypothesis developed at the beginning of the study. Two different contact models, namely the frictional contact model and the bonded contact model, produce a different magnitude and distribution of von Mises stress on the plate used. The frictional contact model seems to be more suitable for initial plate placement conditions where the two fractured bones have not yet fused, while the bonded contact model is more suitable for fracture conditions where the bones have started to fuse. Furthermore, the influence of the screw mounting angle on the analysis results are not yet known so further studies still need to be carried out.

Acknowledgments

The research was supported by *Penelitian Dasar Unggulan Perguruan Tinggi No. 43/UN11.2.1/PT.01.03/DPRM/2021*, Ministry of Education and Culture, Indonesia.

References

[1] Maulana, R. (2015). Tibia stress fracture, Jurnal Kedokteran Syiah Kuala, 15(1), pp. 60-65.
[2] Soni, A. Gupta, R., Gupta, S., Kansay, R., and Kapoor, L. (2019). Mechanism of injury based classification of proximal tibia fractures, Journal of Clinical Orthopaedics and Trauma, 10(4), pp. 785-788. DOI: 10.1016/j.jcot.2018.08.012.
[3] Taheri, E., Sepehri, B., and Ganji, R. (2012). Mechanical validation of perfect tibia 3D model using computed tomography scan, Journal of Engineering, 04(12), pp. 877-880. DOI: 10.4236/eng.2012.412111.
[4] Thakur, A.J. (2012). The Element of Fracture Fixation. India.
[5] Morwood, M. P., Gebhart, S. S., Zamith, N., and Mir, H. R. (2019). Outcomes of fixation for periprosthetic tibia fractures around and below total knee arthroplasty, Journal of Injury, 50(4), pp. 978-982. DOI: 10.1016/j.injury.2019.03.014.
[6] Hiranda, A., Nora, H., Fonna, S., and Huzni, S. (2019). Studi pengaruh element size pada analisis elemen hingga terhadap distribusi tegangan pada kasus fraktur tulang tibia, Seminar Nasional Inovasi Produk Penelitian Pangapdian Masyarakat dan Tantangan Era Revolusi Industri 4.0, Proseding Mutidisplin Ilmu, 2(1), pp. 252-257.
[7] Mischler, S., and Muńoz, A. I. (2013). Wear of CoCrMo alloys used in metal-on-metal hip joints: A tribocorrosion appraisal, Journal of Wear, 293, pp. 1081-1094. DOI: 10.1016/j.wear.2012.11.061.
[8] Guo, Z., Pang, X., Yan, Y., Gao, K., Volinsky, A. A., and Zhang, T. Y. (2015). CoCrMo alloy for orthopedic implant application enhanced corrosion and tribocorrosion properties by nitrogen ion implantation, Journal of Applied Surface Science, 347, pp. 23-34. DOI: 10.1016/j.apsusc.2015.04.054.
[9] Mugnai, R., Tarallo, L., Capra, F., and Catani, F. (2018). Biomechanical comparison between stainless steel, titanium and carbon-fiber reinforced polyetheretherketone volar locking plates for distal radius fractures, Journal of Orthopaedics and Traumatology: Surgery and Research, 104(6), pp. 877-882. DOI: 10.1016/j.otsr.2018.05.002.
[10] Katthagen, J. C., Schwarze, M., Warnhoff, M., Voigt, C., Hurschler, C., and Lill, H. (2016). Influence of plate material and screw design on stiffness and ultimate load of locked plating in osteoporotic proximal humeral fractures, Journal of Injury, 47(3), pp. 617-624. DOI: 10.1016/j.injury.2016.01.004.
[11] Hak, D. J., Banegas, R., Ipaktchi, K., and Mauffrey, C. (2018). Evolution of plate design and material composition, Journal of Injury, 49, pp. S8-S11. DOI: 10.1016/S0020-1383(18)30295-X.
[12] Manivasagam, G., Dhinasekaran, D., and Rajamanickam, A. (2010). Biomedical implants: corrosion and its prevention-a review, Journal of Recent Patents on Corrosion Science, 2(1), pp. 40-54. DOI: 10.2174/1877610801002010040.

[13] Kim, S., Chang, S., and Jung, H. (2010). The finite element analysis of a fractured tibia applied by composite bone plates considering contact conditions and time-varying properties of curing tissues, Journal of Composite Structures, 92(9), pp. 2109-2118. DOI: 10.1016/j.compstruct.2009.09.051.

[14] Kim, S., Chang, S., and Son, D. (2011). Finite element analysis of the effect of bending stiffness and contact condition of composite bone plates with simple rectangular cross-section on the bio-mechanical behaviour of fractured long bones, Journal of Composites Part B: Engineering, 42(6), pp. 1731-1738. DOI: 10.1016/j.compositesb.2011.03.001.

[15] Kim, H., Kim, S., and Chang, S. (2011). Bio-mechanical analysis of a fractured tibia with composite bone plates according to the diaphyseal oblique fracture angle, Journal of Composites Part B: Engineering, 42(4), pp. 666-674. DOI: 10.1016/j.compositesb.2011.02.009.

[16] Nubly, M. H., and Yudo, H. (2017). Strength analysis of propeller shafting on orca class fisheries inspection boat using finite element method, Journal of Civil Engineering and Technology, 8(10), pp. 1599-1610.

[17] Maharaj, P. S., Maheswaran, R., and Vasanthanathan, A. (2013). Numerical analysis of fractured femur bone with prosthetic bone plates, International Conference on Design and Manufacturing, IconDM 2013, Procedia Engineering, 64, pp. 1242-1251. DOI: 10.1016/j.proeng.2013.09.204.

[18] Cao, Y., Zhang, Y., Huang, L., and Huang, X. (2019). The impact of plate length, fibula integrity and plate placement on tibial shaft fixation stability: A finite element study, Journal of Orthopaedic Surgery and Research, 14(1), pp. 1-7. DOI: 10.1186/s13018-019-1088-y.

[19] Chuan, T. K., Hartono, M., and Kumar, N. (2010). Anthropometry of the singaporean and indonesian populations, Journal of Industrial Ergonomics, 40(6), pp. 757-766. DOI: 10.1016/j.ergon.2010.05.001.

[20] Wu, J., and Lee, R. (1997). The advantages of triangular and tetrahedral edge elements for electromagnetic modeling with the finite-element method, IEEE Transactions on Antennas and Propagation, 45(9), pp. 1431-1437.

[21] Das, S., and Sarangi, S. K. (2014). Finite element analysis of femur fracture fixation plates, Journal of Basic and Applied Biology, 1(1), pp. 1-5.

[22] Bergmann, G. (ed.), Charité Universitaetsmedizin Berlin. (2008). Orthoload. Available at: http://www.Orthoload.com.